nature cell biology

DOI: 10.1038/ncb1853

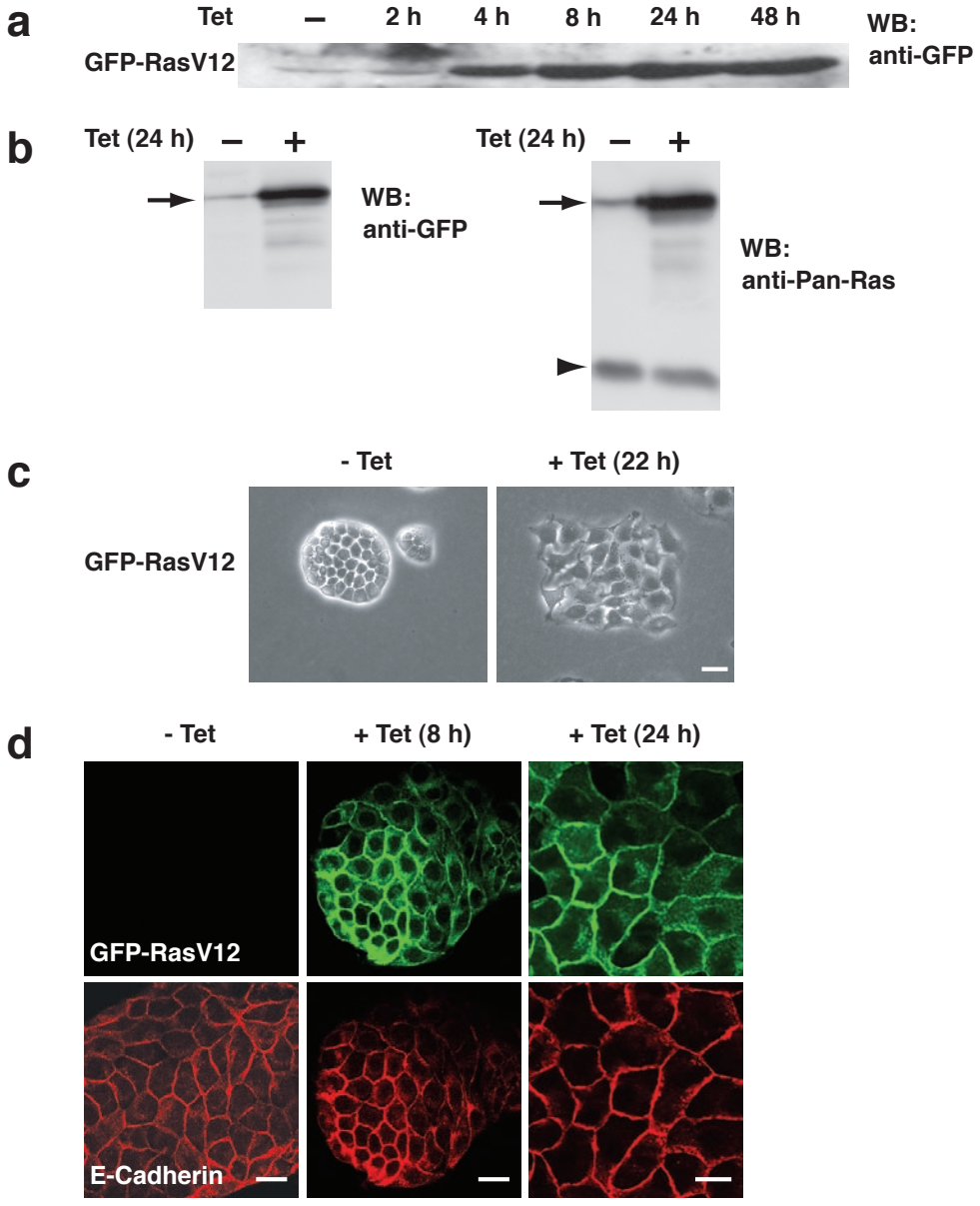

Figure S1 Establishment of a tetracycline-inducible system for GFP-tagged RasV12 in MDCK epithelial cells. **a** Tetracycline-induced expression of GFP-RasV12 protein in MDCK-pTR cells as determined by Western blotting using anti-GFP antibody. **b** Comparison of expression level of exogenous GFP-RasV12 (arrows) and endogenous Ras (arrowhead) proteins. Following 24 h of tetracycline addition, cell lysates of MDCK-pTR GFP-RasV12 cells were examined by Western blotting with anti-GFP and anti-Pan-Ras antibodies. **c** Phase contrast images of MDCK-pTR GFP-RasV12 cells cultured at low density without tetracycline (left) or with tetracycline (right). Scale bar, 10 μm. **d** Confocal images of GFP-RasV12 cells cultured at high density and stained with anti-E-cadherin antibody (red) without or with tetracycline induction (8 h or 24 h). Scale bars, 20 μm.

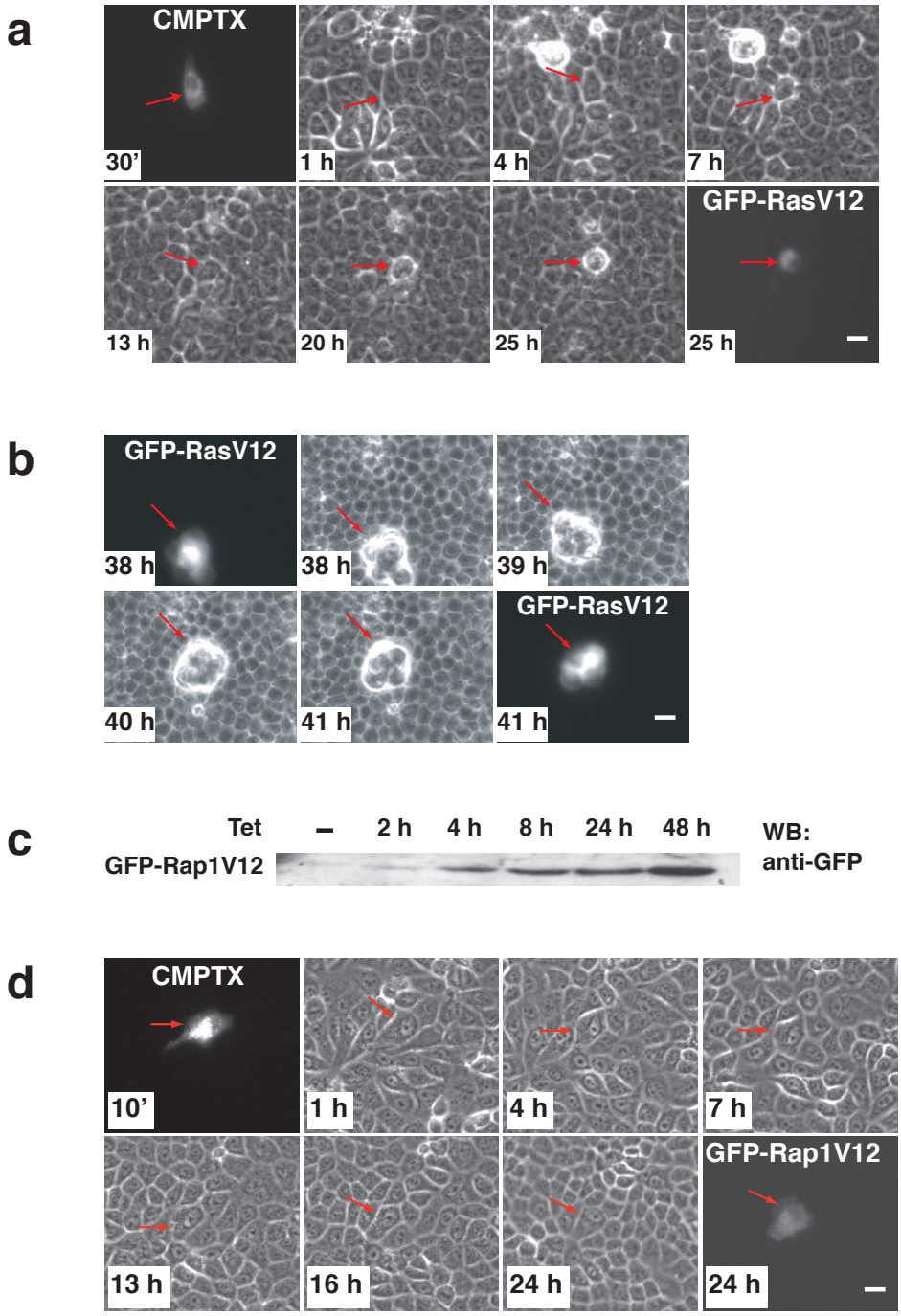

Figure S2 a A single RasV12-expressing cell is extruded from a monolayer of non-transformed cells. Fluorescently labelled MDCK-pTR GFP-RasV12 cells (CMPTX) were cultured with non-transformed MDCK cells at a ratio of 1:100 on collagen gels, followed by tetracycline treatment. Red arrows indicate a fluorescently labelled RasV12 cell. **b** Apically extruded RasV12 cells form multi-cellular aggregates that dynamically move over the apical surface of the non-transformed cells. GFP-RasV12 cells mixed with non-transformed MDCK cells were seeded on collagen. Once a monolayer was formed, RasV12 expression was induced with tetracycline and cells were monitored using time-lapse microscopy. Red arrows indicate RasV12 cells. **c** Tetracycline-induced expression of GFP-Rap1V12 protein in MDCK-pTR cells as determined by Western blotting using anti-GFP antibody. **d** GFP-Rap1V12 cells are not extruded from a monolayer of non-transformed MDCK cells. GFP-Rap1V12 cells were pre-stained with fluorescent dye (CMPTX), and mixed with non-transformed MDCK cells at a ratio of 1:100. Once a monolayer was formed, Rap1V12 expression was induced with tetracycline and cells were monitored using time-lapse microscopy. Red arrows indicate a Rap1V12 cell. **a**, **b**, **d**; Images are extracted from a representative time-lapse analysis. Scale bars, 20 μm.

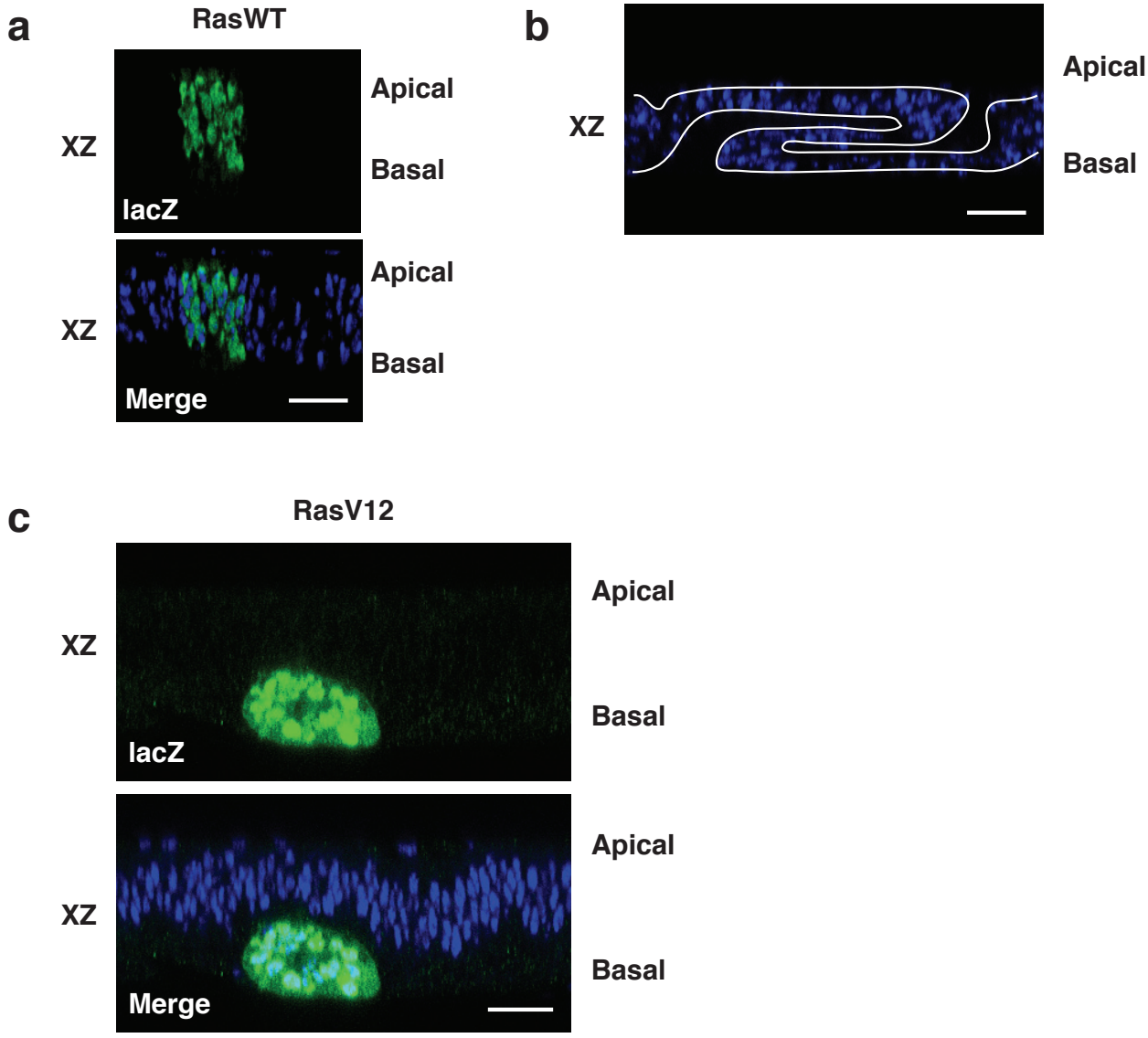

Figure S3 a RasWT-expressing cells are not apically extruded from a normal epithelium *in vivo*. Confocal images of *Drosophila* wing imaginal disc epithelium co-expressing lacZ and RasWT in a mosaic manner. Cells were stained with anti-β-galactosidase antibody (green) and Hoechst (blue). **b** When RasV12 is expressed in the entire epithelium, apical extrusion is not observed and the monolayer becomes irregularly folded. Cells were stained with Hoechst (blue). **c** RasV12-expressing cells are basally delaminated from a normal epithelium *in vivo*. Confocal images of *Drosophila* wing imaginal disc epithelium co-expressing lacZ and RasV12 in a mosaic manner. Cells were stained with anti-β-galactosidase antibody (green) and Hoechst (blue). **a-c**; scale bars, 20 μm.

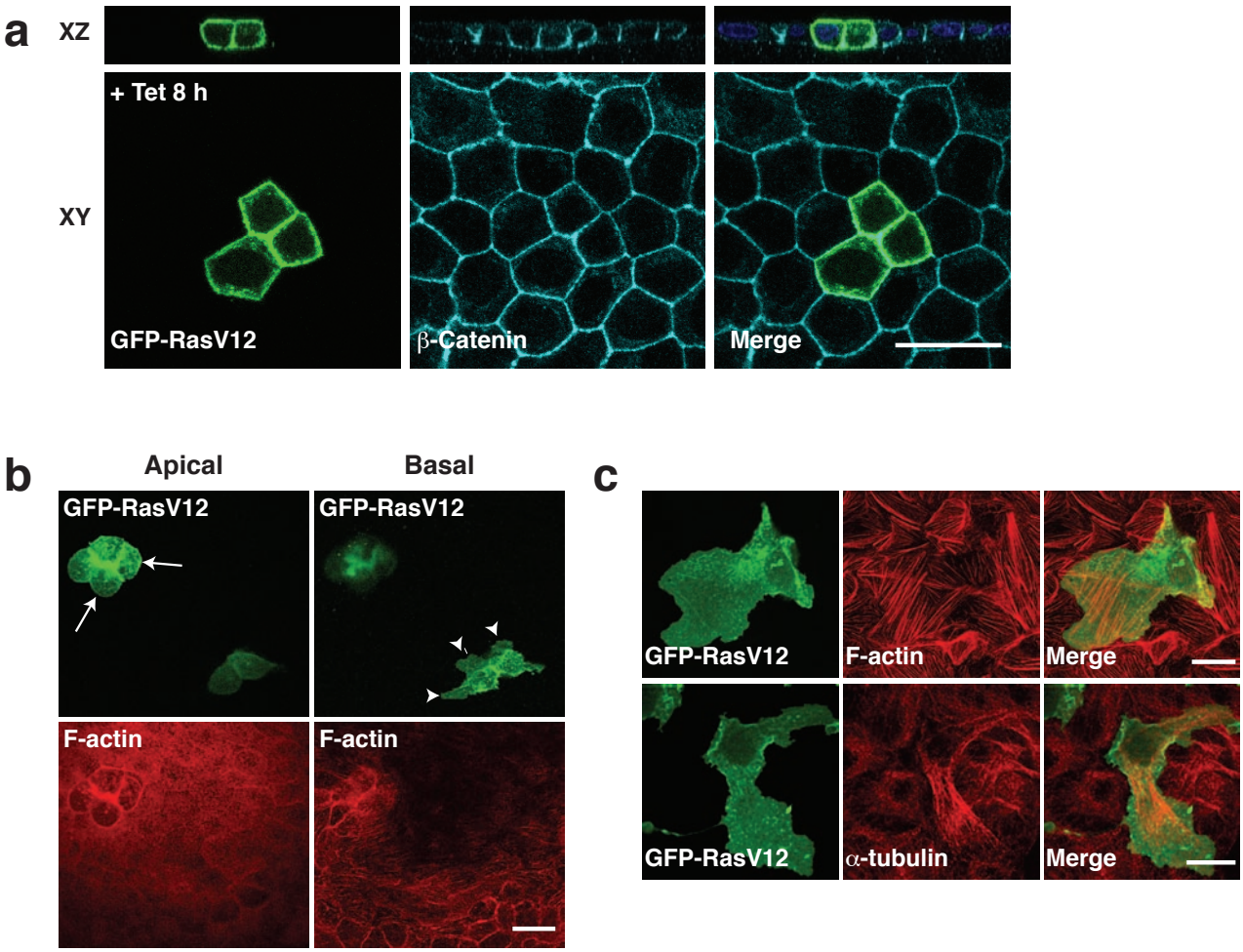

Figure S4 a E-cadherin-based adherens junctions are maintained between GFP-RasV12 cells in a monolayer of normal cells. Confocal images of GFP-RasV12 cells in a monolayer of non-transformed cells. Following 8 h of tetracycline addition, cells were stained with anti-β-catenin antibody (cyan). **b** Apical and basal confocal images of GFP-RasV12 cells in a monolayer of normal MDCK cells on collagen gels. Following 24 h of tetracycline addition, cells were stained with TRITC-phalloidin (red). White arrows indicate apically extruded RasV12 cells. White arrowheads indicate RasV12 cells that have formed basal protrusions. **c** Confocal images of GFP-RasV12 cells in a monolayer of non-transformed cells. Following 24 h of tetracycline addition, cells were stained with TRITC-phalloidin (top panels) or anti-α-tubulin antibody (bottom panels). **a-c**; scale bars, 20 μm.

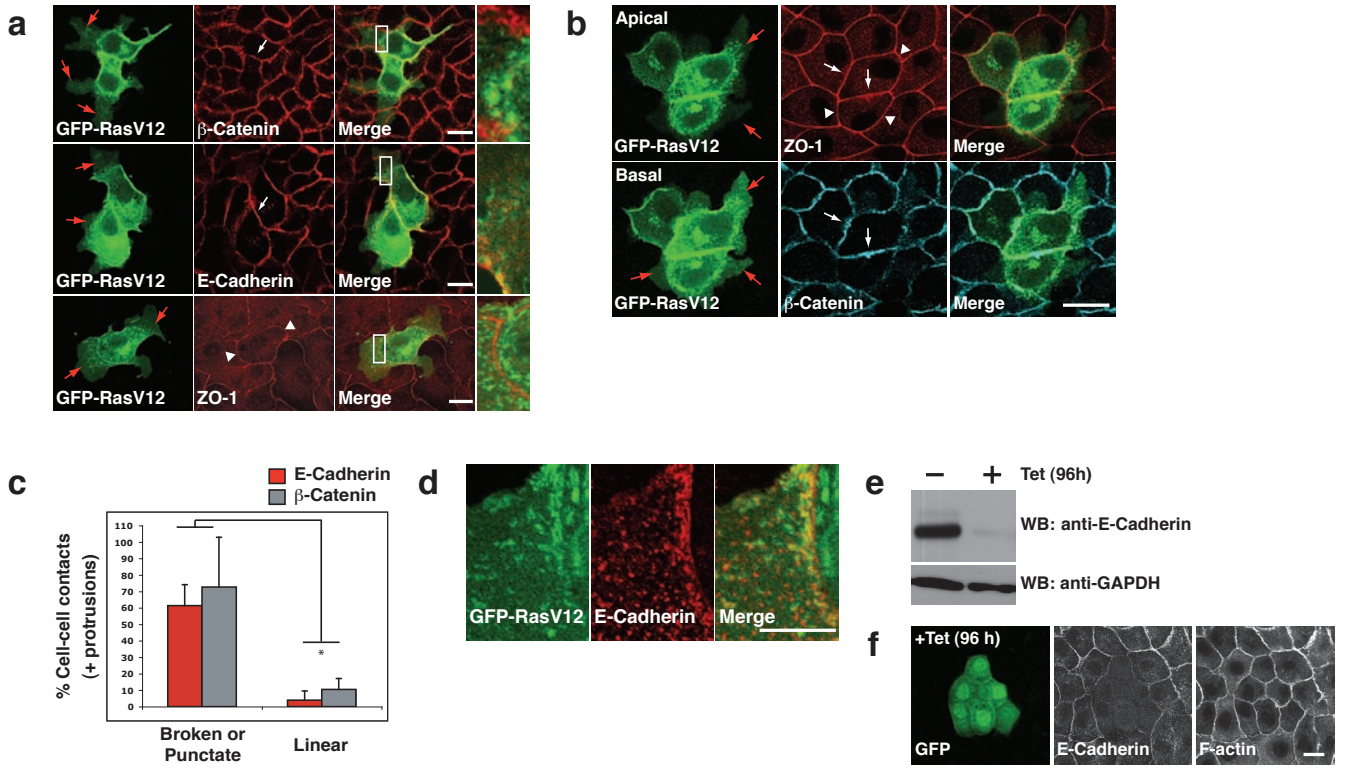

Figure S5 Protrusion formation at the interface between RasV12 and non-transformed cells is associated with disruption of adherens junctions. **a, b** Confocal images of GFP-RasV12 cells mixed with non-transformed cells. Following 8 h incubation with tetracycline, adherens junctions were analysed using anti-E-cadherin and anti-β-catenin antibodies. Tight junctions were analysed using anti-ZO-1 antibody. Red arrows indicate protrusions. White arrows and arrowheads indicate cell-cell contacts between RasV12 cells and those between RasV12 and normal cells where basal protrusions were formed, respectively. The area in the white box of each merge image in **a** is shown in higher magnification on the right. It should be noted that in **b**, cells were double-stained for ZO-1 and β-catenin. **c** Quantification of cell-cell contacts with disrupted (broken or punctate) or linear localisation of E-cadherin (red bar) or β-catenin (grey bar) between normal and RasV12 cells that form protrusions. Values represent mean ± s.d. $*P < 0.05$. **d** Confocal images representing magnified view of a protrusion at the interface between GFP-RasV12 and non-transformed cells. Following 8 h incubation with tetracycline, cells were stained with anti-E-cadherin antibody (red). **e** MDCK cells stably expressing E-cadherin shRNA in a tetracycline-inducible manner. Knockdown of E-cadherin protein was detected by Western blotting using anti-E-cadherin antibody, following 96 h of tetracycline addition. Equal protein loading was confirmed using anti-GAPDH antibody. **f** Knockdown of E-cadherin protein does not lead to protrusion formation in a monolayer of normal cells. GFP is constitutively expressed in E-cadherin shRNA cells. F-actin at cell-cell contacts was labelled using TRITC-phalloidin. **a**, **b**, **d**, **f**; scale bars, 20 μm.

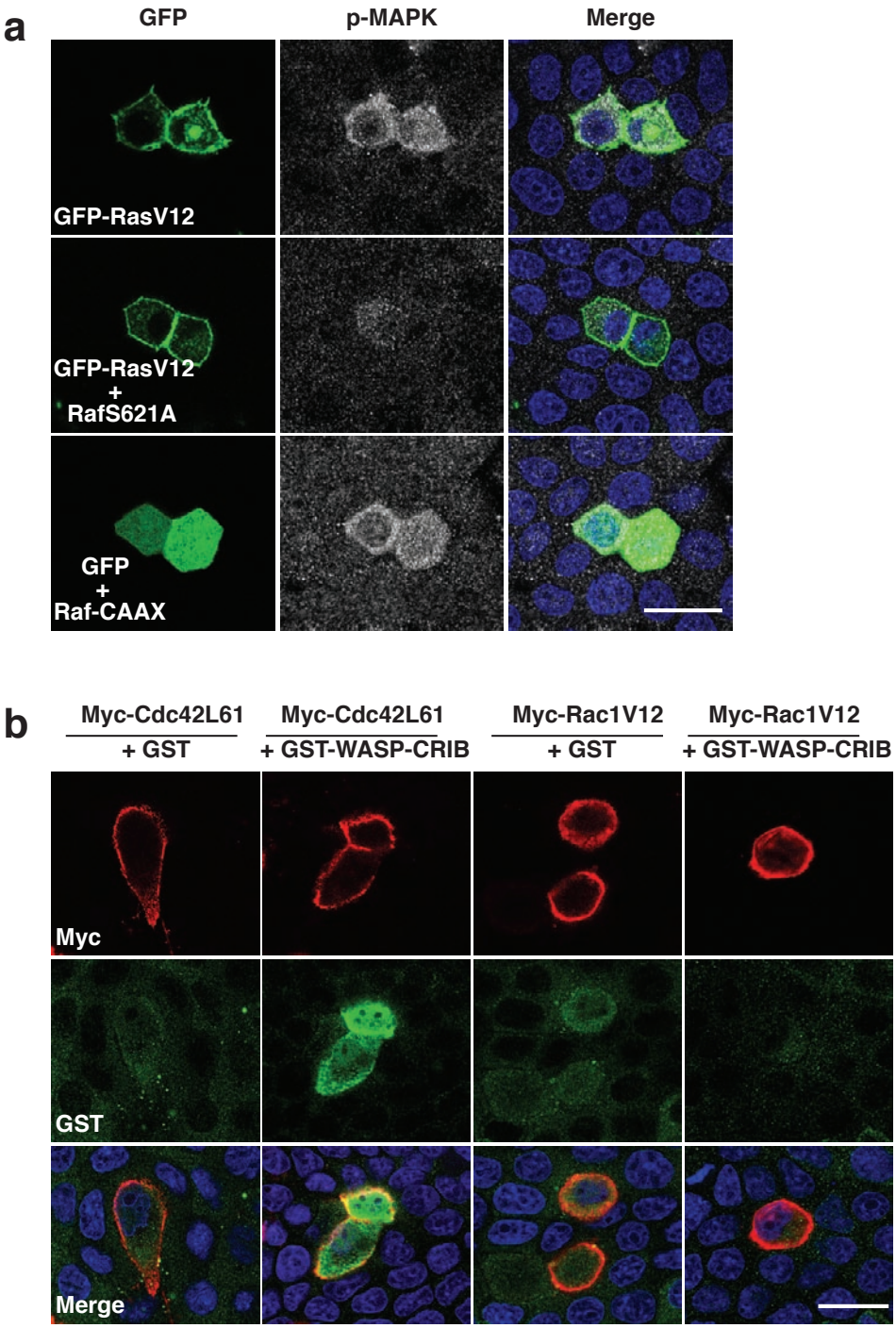

Figure S6 a Confocal images of MDCK cells transiently expressing GFP-RasV12 (top), GFP-RasV12 and dominant negative Raf (RafS621A) (middle), or GFP and dominant active Raf (Raf-CAAX) (bottom). Active MAPK was detected using anti-phospho-MAPK antibody (grey), and nuclei were stained with Hoechst (blue). **b** The Cdc42-binding domain (CRIB domain) of WASP protein specifically binds to GTP-bound Cdc42 but not to GTP-bound Rac1. Confocal images of MDCK cells transiently expressing constitutively active Cdc42 (Myc-Cdc42L61) or Rac1 (Myc-Rac1V12). Fixed cells were incubated with GST or GST-WASP-CRIB protein, followed by immunostaining with anti-GST (green), anti-myc (red) antibodies and Hoechst (blue). **a**, **b**; scale bar, 20 μm.

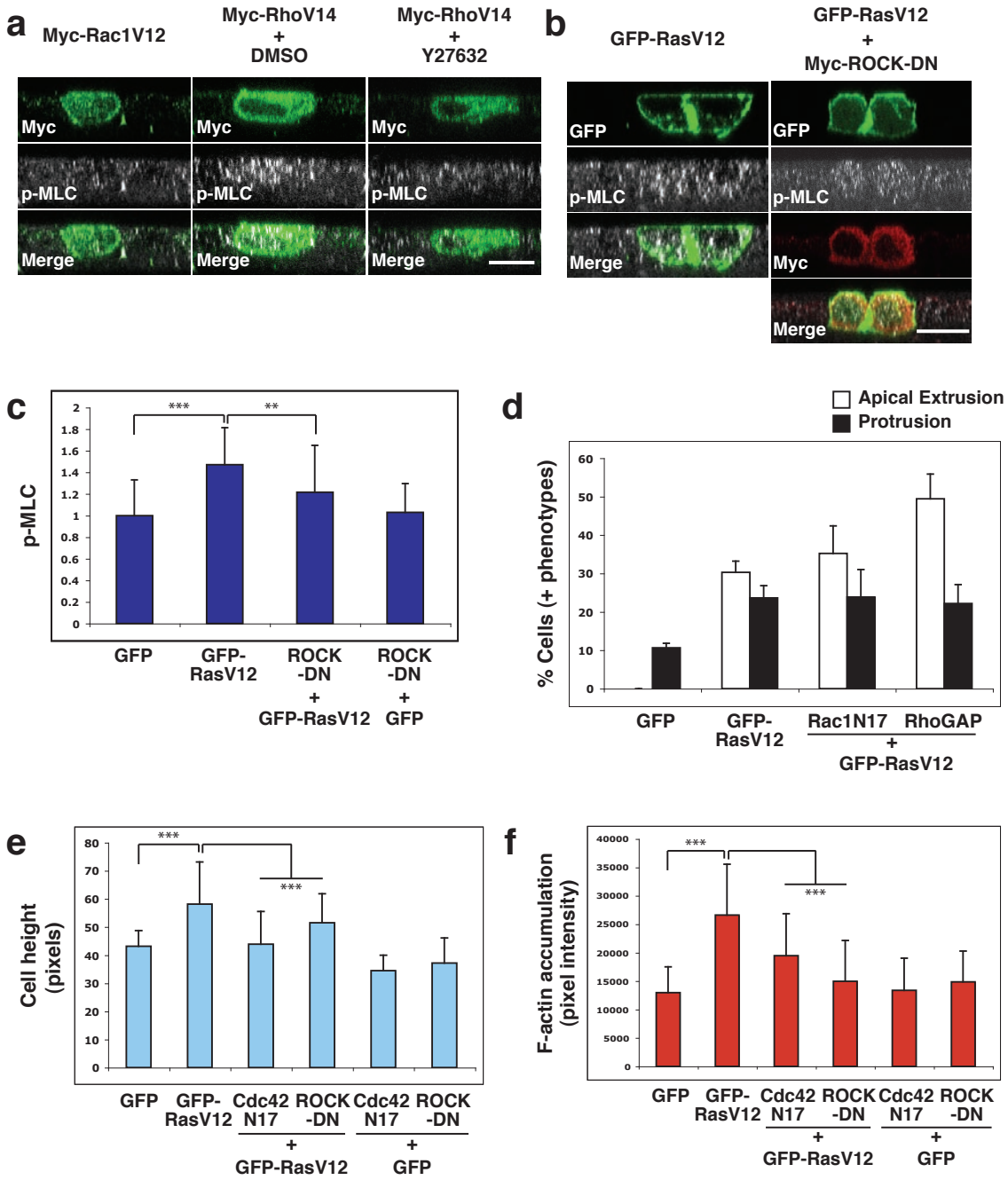

Figure S7 Molecular mechanisms for apical extrusion and basal protrusion formation of RasV12 cells using a transient expression system. **a** Confocal images of MDCK cells transiently expressing constitutively active Rac1 (Myc-Rac1V12) or RhoA (Myc-RhoV14). RhoA-expressing cells were incubated with or without ROCK inhibitor Y27632. Fixed cells were stained with anti-myc (green) and phospho-MLC (grey) antibodies. These results suggest specific immunostaining of phospho-MLC. **b** Confocal images of MDCK cells transiently expressing GFP-RasV12 with or without dominant negative ROCK (Myc-ROCK-DN). Fixed cells were stained with anti-myc (red) and phospho-MLC (grey) antibodies. **c** Quantification of immunofluorescence of phosphorylated myosin light chain (p-MLC) in MDCK cells that transiently express GFP or GFP-RasV12 with or without dominant negative ROCK (ROCK-DN). Values are expressed as a ratio relative to those in GFP-transfected cells, and represent mean ± s.e.m. $^{***}P < 0.0001$ $^{**}P < 0.005$. **d** Quantification of apical extrusion (white bar) and basal protrusion formation (black bar) of MDCK cells that transiently express GFP- or GFP-RasV12 with or without constitutively inactive Rac1 (Rac1N17) or RhoGAP. Values represent mean ± s.e.m. It should be noted that expression of constitutively inactive RhoN19 was toxic for MDCK cells and could not be used for analyses. **e, f** Quantification of **e** cell height or **f** intercellular F-actin of MDCK cells that transiently express GFP or GFP-RasV12 with or without constitutively inactive Cdc42 (Cdc42N17) or ROCK-DN. Values represent mean ± s.d. $^{***}P < 0.0001$. **a**, **b**; Scale bars, 20 μm.

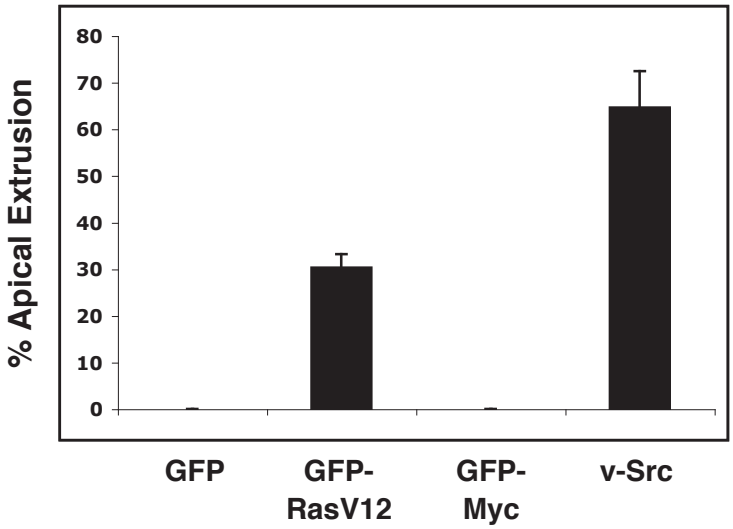

Figure S8 Quantification of apical extrusion of MDCK cells that transiently express GFP-, GFP-RasV12, GFP-Myc or v-Src. Values represent mean ± s.e.m. Expression of v-Src was monitored by immunofluorescence using anti-phospho-tyrosine antibody. For each construct, more than 50 cells from 2-5 independent experiments were analysed. pmCherrry or pEGFP was cotransfected with pcDNA/TO/GFP-Myc or pSG-v-Src to analyse the formation of basal protrusions. It should be noted that basal protrusion formation was not substantially observed in MDCK cells expressing GFP-Myc or v-Src under these experimental conditions (data not shown). We also found that MDCK cells transiently transfected with pRK5-myc RasV12 and pEGFP formed basal protrusions comparable to those observed in cells expressing GFP-RasV12 (data not shown).

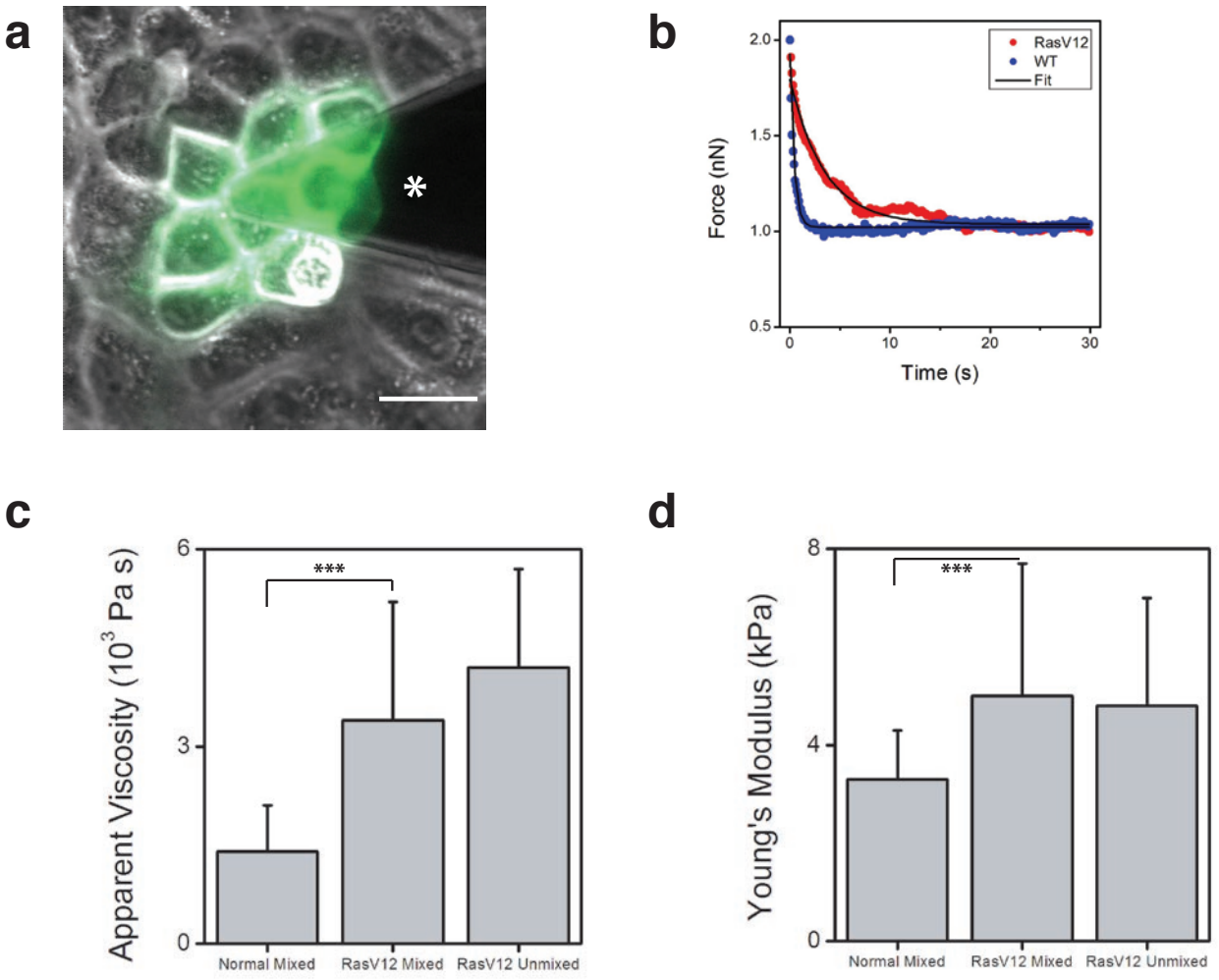

Figure S9 a Simultaneous fluorescence and Atomic Force Microscopy (AFM) allows us to directly visualize the AFM tip (*) and measure the mechanical properties of individual RasV12 cells (green) and the surrounding normal cells. Scale bar; 20 μm. **b** Stress-relaxation tests were performed to measure the apparent cell viscosity (μ). RasV12 cells (red) had a much higher μ than normal cells (blue), which resulted in a slower relaxation time after being indented with 2 nN of force. After fitting the data (black) with a stress-relaxation model for AFM, μ values were determined. **c** Normal cells had a μ which was ~2.5 times smaller than RasV12 cells that were mixed or unmixed with normal cells. Values represent mean ± s.d. ***$P < 0.0001$. **d** Consistent with these results, the local elasticity of the cell membrane was determined from force-indentation measurements and RasV12 cells were found to be ~1.5 times stiffer than normal cells. Values represent mean ± s.d. ***$P < 0.0001$. This was also consistent with the relaxed modulus measured from the stress-relaxation tests (data not shown). **c, d** Normal Mixed; normal cells that were mixed with RasV12 cells. RasV12 Mixed; RasV12 cells that were mixed with normal cells. RasV12 Unmixed; RasV12 cells alone. No significant difference was observed between the values of RasV12 cells that were mixed or not mixed with normal cells.

Fig. S1a and S2c

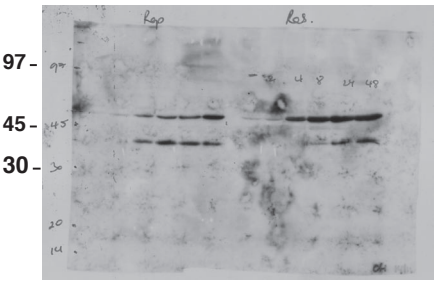

Fig. S1b

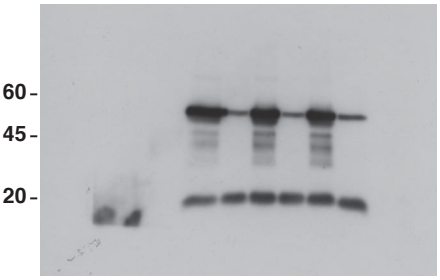

Fig. S1b

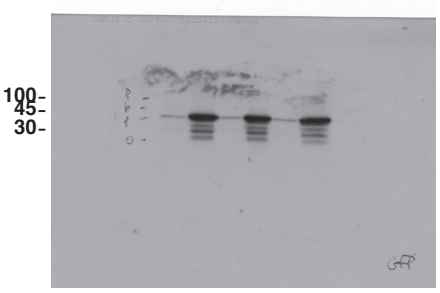

Fig. S5e

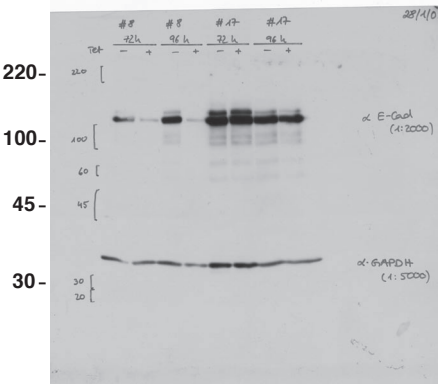

Figure S10 Full scans of western blot data

Supplementary Movies

Movie S1 This movie shows the extrusion of GFP-RasV12 cells from a monolayer of normal MDCK cells, seeded on collagen gels. GFP-RasV12 cells were pre-stained with fluorescent dye and mixed with normal MDCK cells at a ratio of 1:100. Once a monolayer was formed, GFP-RasV12 expression was induced with tetracycline at the beginning of the experiment. Once extruded, the RasV12 cells remain viable and proliferate to form a multi-cellular aggregate that loosely attaches to and moves above the normal MDCK monolayer. Time-lapse images were captured at 10-min intervals for 48 h, with fluorescent images captured every 30 min. (QuickTime; 3 MB)

Movie S2 This movie shows that a GFP-Rap1V12-expressing MDCK cell is not extruded from a monolayer of normal MDCK cells on collagen gels. GFP-Rap1V12 cells were pre-stained with fluorescent dye and mixed with normal MDCK cells at a ratio of 1:100. Once a monolayer was formed, GFP-Rap1V12 expression was induced with tetracycline at the beginning of the experiment. Time-lapse images were captured at 10-min intervals for 24 h, with fluorescent images captured every 30 min. (QuickTime; 2.7 MB)

Movie S3 This movie shows that GFP-RasV12 MDCK cells are not extruded from a monolayer of GFP-RasV12 MDCK cells on collagen gels. GFP-RasV12 cells were pre-stained with fluorescent dye and mixed with non-stained GFP-RasV12 cells at a ratio of 1:100. Once a monolayer was formed, GFP-RasV12 expression was induced with tetracycline at the beginning of the experiment. Time-lapse images were captured at 10-min intervals for 24 h, with fluorescent images captured every 30 min. (QuickTime; 1.2 MB)

Movie S4 This movie shows that a non-extruded GFP-RasV12 cell in a monolayer of normal MDCK cells forms dynamic basal protrusions. GFP-RasV12 cells were pre-stained with fluorescent dye and mixed with normal MDCK cells at a ratio of 1:100. Once a monolayer was formed, GFP-RasV12 expression was induced with tetracycline at the beginning of the experiment. Time-lapse images were captured at 10-min intervals for 24 h, with fluorescent images captured every 50 min. (QuickTime; 136 KB)

Supplementary Discussion

First, we would like to discuss the molecular mechanism of apical extrusion of RasV12 cells. We have not observed F-actin accumulation at the interface between normal and RasV12 cells (Fig. 2a and d), indicating that apical extrusion of RasV12 cells is not induced by "squeezing out" from the surrounding cells as observed in apical extrusion of apoptotic cells[1]. The PI3 kinase pathway is involved in lamellipodia formation and PI3K inhibitor does not affect apical extrusion (Fig. 2f), suggesting that apical extrusion is not due to increased migration of RasV12 cells. Then, how are RasV12 cells apically extruded when surrounded by normal cells?

By analysing RasV12 cells that have not yet been extruded and have remained in the monolayer of normal cells, we have found that phosphorylation of myosin light chain is enhanced in RasV12 cells (Fig. 2c; Supplementary Information, Fig. S7b and c) and that F-actin is accumulated at the intercellular junctions between RasV12 cells (Fig. 2a and d; Supplementary Information, Fig. S7f). Activation of myosin-II and intercellular F-actin accumulation would enhance surface tension and cell-cell adhesions of RasV12 cells, respectively[2]. Interestingly, these two parameters have been reported to be involved in cell sorting[2-6]; cells with higher surface tension and/or intercellular adhesions are thermodynamically encompassed by cells with lower tension and/or adhesions. Thus, the modulation of cytoskeleton that we have observed in RasV12 cells would promote RasV12 cells to self-aggregate in a monolayer of normal cells as a physically favoured process. We

have also observed that the height of RasV12 cells is enhanced when surrounded by normal cells (Fig. 2a and b), indicating that forces along the apico-basal axis are generated inside RasV12 cells. Since the presence of matrix on the basal side physically blocks basal movement of RasV12 cells, forces toward the apical direction will drive RasV12 cells to be apically extruded.

We have further investigated the physical properties of normal and RasV12 cells by using Atomic Force Microscopy (AFM)(Supplementary Information, Fig. S9). Utilising simultaneous AFM and fluorescence microscopy (Supplementary Information, Fig. S9a), we have directly measured the apparent cell viscosity (μ) and the membrane elasticity (or Young's Modulus)(E) of RasV12 and surrounding normal cells. We have found that RasV12 cells have significantly greater μ (Supplementary Information, Fig. S9b and c) and E values (Supplementary Information, Fig. S9d) than the surrounding normal cells do, indicating that RasV12 cells are stiffer and more viscous than normal cells. These parameters in RasV12 cells in a monolayer of normal cells are not significantly different from those in RasV12 cells in a monolayer of RasV12 cells, suggesting that these physical properties are regulated in a cell-autonomous fashion. Notably, these mechanical parameters are significant in determining cell packing and geometry according to the recently proposed vertex model for cell organisation within an epithelial monolayer[7]. Based on this recent model, we suggest that energetic driving forces may play a vital role in the aggregation (and possibly extrusion) of RasV12 cells within the normal cell monolayer.

In Supplementary Information, Fig. S5, we present our analyses on cell-cell contacts at the interface between RasV12 and non-transformed cells. Components of adherens junctions, E-cadherin, β-catenin and p120-catenin, show incomplete or punctate immunostaining at cell-cell contacts where RasV12 cells extend a protrusion (Supplementary Information, Fig. S5a-c; data not shown for p120). Frequently, E-cadherin and β-catenin localise in vesicular puncta within the protrusion (Supplementary Information, Fig. S5d; data not shown for β-catenin). Localisation of tight junction protein ZO-1 is not affected by protrusion formation (Supplementary Information, Fig. S5a and b, white arrowheads), indicating that E-cadherin-based cell-cell contacts are specifically disrupted. Both adherens junctions and tight junctions are maintained between RasV12 cells (Supplementary Information, Fig. S5a and b, white arrows), suggesting that loss of E-cadherin-based cell-cell adhesion specifically occurs at the interface between RasV12 and non-transformed cells. We therefore ask whether loss of E-cadherin is sufficient to induce protrusion formation by knocking down E-cadherin protein in MDCK cells using a tetracycline-inducible shRNA system (Supplementary Information, Fig. S5e). No protrusion formation is observed at the interface between normal and E-cadherin-deficient MDCK cells (Supplementary Information, Fig. S5f), indicating that loss of E-cadherin alone does not lead to protrusion formation but additional Ras-mediated signalling is required.

We show in Fig. 4c that ROCK and Cdc42 are crucial in determining the fate of RasV12 cells in a monolayer of normal cells; either apically extruded, or

remaining in the monolayer and forming basal protrusions. Expression of dominant negative ROCK suppresses RasV12-induced phosphorylation of myosin light chain (Supplementary Information, Fig. S7b and c), suggesting its role in activation of myosin-II. However, we cannot exclude the possibility that other pathways may also be involved in the regulation of myosin-II. ROCK can be activated by active Rho[8-10]. Interestingly, expression of p50RhoGAP, an inactivator of Rho[11], significantly enhances apical extrusion of RasV12 cells (Supplementary Information, Fig. S7d), suggesting that some Rho downstream targets play a negative role in this process. It is feasible that Rho activity may be regulated locally or temporally, which affects its multiple downstream targets and the fate of RasV12 cells. In future studies, it remains to be clarified how the activity of ROCK and Cdc42 is regulated in RasV12 cells surrounded by normal cells.

E-cadherin knockdown in cells surrounding RasV12 cells reduces the frequency of apical extrusion, while promoting basal protrusion formation and invasion (Fig. 5a-c). In addition, other data suggest that signalling pathways of surrounding normal cells can affect the behaviour of RasV12 cells. Expression of dominant negative Raf has no effect on the frequency of basal protrusion formation of RasV12 cells in a monolayer of normal cells (Fig. 4b), whereas addition of MEK inhibitor suppresses it (Fig. 3e). Expression of dominant negative ROCK substantially promotes protrusion formation of RasV12 cells (Fig. 4c), whereas addition of blebbistatin does not affect it (Fig. 3e). These data

indicate the involvement of basal activity of MEK and myosin-II of surrounding normal cells in this process. Collectively, our results suggest that the fate of RasV12 cells in a monolayer of normal cells is determined by the total balance of multiple signalling pathways in both RasV12 cells and surrounding normal cells. It is highly plausible that apical extrusion would suppress tumour formation and that basal protrusion formation and basal delamination would promote it. We expect that novel therapeutic treatment for cancer may be discovered by further studying the molecular mechanisms of apical extrusion and basal protrusion formation of transformed cells.

Finally, in MDCK cells, we have found that expression of v-Src highly promotes apical cell extrusion (Supplementary Information, Fig. S8), but not basal protrusion formation (data not shown). Apical extrusion is observed in cells expressing either RasV12 or v-Src that stimulate distinct downstream targets. Therefore, it will be interesting to investigate whether common signalling pathways are involved in these processes. Overexpression of Myc induces neither apical extrusion nor basal protrusion formation (Supplementary Information, Fig. S8, and data not shown). These data suggest that different oncogenic stimuli induce different phenomena between normal and transformed cells, as previously shown in *Drosophila melanogaster*[12, 13]. In future studies, it should be examined whether deregulation of other oncoproteins or tumour suppressor proteins induces distinct phenomena at the interface with normal cells and how those phenomena are involved in the early stage of carcinogenesis in vertebrates.

Supplementary Methods

Plasmids. pcDNA/TO/GFP was constructed as described previously[14]. cDNAs of H-RasV12 and Rap1V12 were amplified by PCR from pRK5-myc-H-RasV12 and pRK5-myc-Rap1V12 respectively, and were then cloned into an EcoRI site of pcDNA/TO/GFP. Similarly, cDNA of c-myc was amplified by PCR from MSCV-hmyc-IRES-GFP, and cloned into EcoRI/Xho sites of pcDNA/TO/GFP. pcDNA6/TR and pcDNA4/TO were obtained from Invitrogen. pRK5-myc-H-RasV12, pRK5-myc-Rap1V12, pRK5-myc-Cdc42N17, pRK5-myc-Cdc42L61, pBOS-myc-Rac1N17, pBOS-myc-Rac1V12, pBOS-myc-RhoV14, and pGEX-2T-p50RhoGAP catalytic domain were all kindly provided by A. Hall (Memorial Sloan-Kettering Cancer Center, NY). pLXSN-myc-p110-CAAX was kindly provided by A. Lloyd (University College London, London). MSCV-hmyc-IRES-GFP was provided by S. Lowe (Cold Spring Harbor Laboratory, NY). pEGFP, pCMV-Raf-CAAX and pCMV-RafS621A were from Clontech (Mountain View, CA). pCAGGS-myc-ROCK1 Δ3 KD (ROCK-DN) was kindly provided by E. Sahai (Cancer Research UK, London). To construct pcDNA/TO/Cherry p50RhoGAP catalytic domain, the cDNA of p50RhoGAP catalytic domain was amplified from pGEX-2T-p50RhoGAP catalytic domain by PCR, and inserted into the EcoRI/NotI site of pcDNA/TO/Cherry. To obtain pcDNA/TO/Cherry, the cDNA of mCherry was amplified from pmCherry C1 by PCR, and was inserted into the EcoRI/BamHI site of pcDNA/TO. pmCherry C1 was a generous gift from

R. Y. Tsien (University of California at San Diego, CA). pSG-v-Src was described previously[15].

Cell culture and RNA interference. MDCK cells were cultured in Dulbecco's modified Eagle's medium (DMEM) supplemented with 10% fetal calf serum (FCS) and penicillin/streptomycin at 37°C and ambient air supplemented with 5% CO_2. To establish MDCK cells stably expressing GFP-RasV12 in an inducible manner, a Tet-ON system was used. Briefly, MDCK cells were transfected with pcDNA6/TR using Lipofectamine^{TM} 2000 (Invitrogen), followed by selection in medium containing 5 μg ml^{-1} of blasticidin (Invitrogen). pcDNA4/TO/GFP-RasV12 was then used for the second transfection and the doubly transfected cells were selected in medium containing 10% FCS (tetracycline-free) (PAA Laboratories, Pasching, Austria), 5 μg ml^{-1} of blasticidin and 400 μg ml^{-1} of zeocin (Invitrogen). MDCK cells stably expressing GFP and GFP-Rap1V12 were produced under the same conditions. To induce GFP, GFP-RasV12 and GFP-Rap1V12 expression, 2 μg ml^{-1} tetracycline was added to culture medium. After the establishment of the RasV12 cell line, we confirmed that the expression level of GFP-RasV12 was uniform between cells as follows; we plated RasV12 cells sparsely and established more than 30 independent clones isolated from single cells. By comparing the expression of GFP-RasV12 between the clones by

Western blotting, we confirmed that GFP-RasV12 is indeed expressed at the same level in the RasV12 cell line we have used for the experiments.

For transient expression experiments (Fig. 4a-c; Supplementary Information, Fig. S6-8), MDCK cells were first seeded on collagen-coated coverslips in 6-well culture dishes (Nunc, Roskilde, Denmark) at a density of 7 x 10^5 cells per well. On the following day, cells were transiently transfected with the indicated constructs (2 μg per construct) using Lipofectamine™ 2000 (Invitrogen) according to manufacturer's instructions. After 24 h of transfection, cells were fixed and immunostained as described below. In Supplementary Information, Fig. S7a, following 4 hr of transfection, MDCK cells transiently transfected with constitutively active Rho (Myc-RhoV14) were further incubated with or without Y27632 for 18 h.

MDCK cells stably expressing E-cadherin shRNA in a tetracycline-inducible manner were produced as follows; E-cadherin shRNA oligonucleotides (E-Cad shRNA-1; 5'-GATCCCCGGACGTGGAAGATGTGAATTTCAAGAGAATTCACATCTTCCACGTCCTTTTTGGAAA-3' and 5'-AGCTTTTCCAAAAAGGACGTGGAAGATGTGAATTCTCTTGAAATTCACATCTTCCACGTCCGGG-3', and E-Cad shRNA-2; 5'GATCCCCGTCTAACAGGGACAAAGAATTCAAAGAGATTCTTTGTCCCTGTTAGACTTTTTC-3' and 5'-

TCGAGAAAAAGTCTAACAGGGACAAAGAATCTCTTGAATTCTTTGTCC CTGTTAGACGGG-3')[16] were cloned into BglII and XhoI sites of pSUPERIOR.neo+gfp (Oligoengine, Seattle, WA). MDCK-pTR cells were transfected with pSUPERIOR.neo+gfp E-cadherin shRNA using Metafectene ^{TM}Pro (Biontex, Germany), followed by selection in medium containing 5 μg ml^{-1} of blasticidin and 800 μg ml^{-1} of G418 (Calbiochem). More than two stable clones were obtained for two independent shRNA oligonucleotides. Knockdown of E-cadherin was analysed by immunofluorescence and Western blotting following 96 h incubation with tetracycline (2 μg ml^{-1}). It should be noted that comparable effect of E-cadherin knockdown on protrusion formation or apical extrusion was observed in cells expressing E-cadherin shRNA-1 or -2.

Cells were plated as described below, except where indicated as low-density cells were plated at 1 x 10^5 cells in 6-well culture dishes.

Immunofluorescence. Immunofluorescence of cells cultured on serum-coated glass coverslips was performed as previously described[17]. Cells cultured on collagen gels were examined using a Leica TCS SPE confocal microscope and Leica Application Suite (LAS) software. Cells cultured on glass coverslips were examined using a Bio-Rad Radiance 2100 MP system mounted on a Nikon 800 microscope using Lasersharp software (Biorad). Images were analysed using ImageJ 1.36b (National Institute of Health) or Volocity software (Improvision).

Cell height (from apical to basal membranes) and F-actin accumulation at cell-cell contacts were both quantified using Metamorph 6.0 digital analysis software (Universal Imaging)(Fig. 2b and d; Supplementary Information, Fig. S7e and f). To determine the level of F-actin at cell-cell contacts, a defined region was created to encompass the area of a cell-cell contact in xz confocal sections. The total pixel intensity within this region (200 pixels) was determined. For quantification of apical extrusion of GFP-RasV12 cells in the presence or absence of inhibitors (Fig. 2f), GFP-RasV12 cells in groups > 3 cells were examined. Minor and major protrusions were counted as less or greater than 10 μm in length, respectively (Fig. 3d). To determine the amount of GST-WASP-CRIB (Fig. 4e) or p-MLC (Supplementary Information, Fig. S7c) in GFP- or GFP-RasV12-expressing cells, Metamorph 6.0 digital analysis software (Universal Imaging) was used. Briefly, a defined region was created in the cytoplasm of the indicated cells in xz confocal sections. For each cell, 5 (for GST-WASP-CRIB) or 8 (for p-MLC) regions were created. The total pixel intensity within each region (73 pixels) was determined and the mean pixel intensity was calculated for each cell. In Fig. 5c, GFP-RasV12 cells or normal MDCK cells that were apically extruded, basally delaminated or formed basal protrusions were counted and expressed as a ratio relative to total cells. Cells were counted following 24 h of tetracycline addition, however MDCK-pTR E-cadherin shRNA cells were incubated with tetracycline for 72 h prior to mixing with other cells to induce sufficient knockdown of E-cadherin protein. In Supplementary Information, Fig. S5c, the correlation between protrusion

formation and E-cadherin or β-catenin mis-localisation was quantified as follows. Cell-cell contacts between RasV12 and normal MDCK cells were first identified using F-actin staining at the contact site. When 50% or less of the contact site was stained with E-cadherin or β-catenin, it was counted as broken or punctate. Conversely, cell-cell contacts with > 80% E-cadherin or β-catenin staining were counted as linear.

Atomic Force Microscopy. A JPK AFM (Nanowizard I) was used for all experiments with MSCT-AUHW cantilevers (14±1 pN/nm). The AFM was mounted on an inverted Olympus IX71 phase contrast and fluorescence microscope for simultaneous optical imaging and mechanical analyses. Force curves were measured at 1 Hz and analysed with the Hertz model to determine cortical elasticity for a 500-nm indentation[18]. Stress-relaxation experiments were performed in constant height mode and the vertical deflection sampled at 10 Hz. Data were fit with a stress-relaxation model (in the limit of a conical indenter) according to previous methodologies[19, 20] to determine the apparent viscosity of the cell.

Statistical analyses. Student's *t* tests were used to determine P value because this test requires variables with no fixed limits.

Fig. 1d: ratios were transformed to arcsin using Excel software, and two-tailed Student's *t* tests were used to determine P value. Control, n = 98 groups of cells; + 4-AP, n = 101 groups of cells. Values represent mean ± s.d. P = 0.31. Fig. 2b: two-tailed Student's *t* tests were used to determine P value. Values represent mean ± s.d. A total of 40-85 cells from three independent experiments were analysed. MDCK vs GFP-RasV12, ***P = 0.00036; GFP-RasV12 vs GFP-RasV12 cells only, ***P = 0.00018. Fig. 2d: two-tailed Student's *t* tests were used to determine P value. Values represent mean ± s.d. A total of 30-60 cell-cell contacts from four independent experiments were analysed. R:R vs R:M, ***P = 1.3×10^{-14}; R:R vs M:M, ***P = 1.2×10^{-17}; R:R vs R:R (RasV12 cells only), ***P = 8.0×10^{-9}. Fig. 2f: the number of RasV12 cell aggregates in which the majority or minority of RasV12 cells were apically extruded was expressed as a ratio relative to that of total RasV12 cell aggregates. RasV12 cells in groups > 3 cells were included in analyses, and one-tailed Student's *t* tests were used to determine P value to compare with DMSO control. In each experiment, ~ 20 groups of RasV12-expressing cells were counted. Values represent mean from 4-5 independent experiments ± s.d. U0126, ***P = 0.00016 for white bar and 2.3×10^{-6} for black bar; Y27632, **P = 0.0041 for white bar and P = 0.11 for black bar; blebbistatin, ***P = 0.00022 for white bar and **P = 0.0012 for black bar; cytochalasin D, ***P = 0.00010 for white bar and *P = 0.026 for black bar. Fig. 3d: ratios were transformed to arcsin using Excel software and two-tailed Student's *t* tests were used to determine P value. Minor or major protrusion formation at cell-cell

contacts, relative to total cell-cell contacts was scored between RasV12 and normal MDCK cells (n= 230) or between RasV12 cells (n= 180). Values represent mean ± s.d. ***P = 4.4×10^{-5}. Fig. 3e: one-tailed Student's *t* tests were used to determine P value to compare with DMSO control. 60-80 groups of cells were analysed for each experimental condition. Values represent mean from 3-4 independent experiments ± s.e.m. U0126, *P = 0.016; LY294002, *P = 0.0070; cytochalasin D, **P = 0.0031. Fig. 4a and b: the number of GFP or GFP-RasV12 cells apically extruded or forming major basal protrusions was expressed as a ratio relative to that of total cells. Two-tailed Student's *t* tests were used to determine P value. In each experiment, 50-150 cells were counted. Values represent mean from more than five independent experiments ± s.e.m. Fig. 4a, ***P = 1.1×10^{-7} for white bar and ***P = 0.00099 for black bar. Fig. 4b, ***P = 9.9×10^{-5} for white bar. Fig. 4c: the number of GFP or GFP-RasV12 cells apically extruded or forming major basal protrusions was expressed as a ratio relative to that of total cells. Two-tailed Student's *t* tests were used to determine P value. In each experiment, 50-115 cells were counted. Values represent mean from more than five independent experiments ± s.e.m. GFP-RasV12 vs Cdc42N17 + GFP-RasV12, ***P = 1.2×10^{-7} for white bar and ***P = 4.1×10^{-8} for black bar; GFP-RasV12 vs ROCK-DN + GFP-RasV12, **P = 3.7×10^{-7} for white bar and **P = 0.0014 for black bar. Fig. 4e: two-tailed Student's *t* tests were used to determine P value. A total of 50-70 cells from three independent experiments were analysed. Values represent mean ± s.e.m. **P = 0.0019 and ***P = 2.7×10^{-8}. Fig. 5c: one-

tailed Student's *t* tests were used to determine P value. Values represent mean from 2-3 independent experiments ± s.d. GFP-RasV12 + E-cadherin shRNA cells, n = 301 cells; MDCK + E-cadherin shRNA cells, n = 396 cells; GFP-RasV12 + MDCK cells, n = 536 cells. *P = 0.040, **P = 0.0026, ***P = 0.00044. Fig. S5c: one-tailed Student's *t* tests were used to determine P values. Values represent mean ± s.d. n = 54 for both E-cadherin and β-catenin. *P = 0.012 for E-cadherin and *P = 0.041 for β-catenin. Fig. S7c: two-tailed Student's *t* tests were used to determine P value. A total of 25-50 cells from three independent experiments were analysed. Values represent mean ± s.e.m. **P = 0.0023 and ***P = 6.4×10^{-9}. Fig. S7d: the number of GFP or GFP-RasV12 cells apically extruded or forming major basal protrusions was expressed as a ratio relative to that of total cells. Two-tailed Student's *t* tests were used to determine P value. In each experiment, 50-150 cells were counted. Values represent mean from more than five independent experiments ± s.e.m. GFP-RasV12 vs Rac1N17+GFP-RasV12, P = 0.62 for white bar, P = 0.98 for black bar; GFP-RasV12 vs RhoGAP+GFP-RasV12, P = 0.037 for white bar, P = 0.81 for black bar. Fig. S7e: two-tailed Student's *t* tests were used to determine P value. Values represent mean ± s.d. A total of 30-160 cells from five independent experiments were analysed. GFP vs GFP-RasV12, ***P = 1.7×10^{-20}; GFP-RasV12 vs Cdc42N17+GFP-RasV12, ***P = 4.7×10^{-17}; GFP-RasV12 vs ROCK-DN+GFP-RasV12, ***P = 6.7×10^{-5}. Fig. S7f: two-tailed Student's *t* tests were used to determine P value. Values represent mean ± s.d. A total of 25-60 cells from four independent experiments were analysed. GFP vs GFP-RasV12,

***P = 1.3 x 10^{-13}; GFP-RasV12 vs Cdc42N17+GFP-RasV12, ***P = 9.8 x 10^{-6}; GFP-RasV12 vs ROCK-DN+GFP-RasV12, ***P = 3.2 x 10^{-8}. Fig. S9: two-tailed Student's *t* tests were used to determine P values. Values represent mean from two independent experiments ± s.d. Normal mixed vs RasV12 mixed ***P = 8.6 X 10^{-5} for apparent viscosity (n = 16), ***P = 1.2 X 10^{-7} for Young's Modulus (n = 15).

References

1. Rosenblatt, J., Raff, M. C. & Cramer, L. P. An epithelial cell destined for apoptosis signals its neighbors to extrude it by an actin- and myosin-dependent mechanism. Curr Biol **11**, 1847-57 (2001).
2. Lecuit, T. & Lenne, P. F. Cell surface mechanics and the control of cell shape, tissue patterns and morphogenesis. Nat Rev Mol Cell Biol **8**, 633-44 (2007).
3. Hayashi, T. & Carthew, R. W. Surface mechanics mediate pattern formation in the developing retina. Nature **431**, 647-52 (2004).
4. Foty, R. A., Pfleger, C. M., Forgacs, G. & Steinberg, M. S. Surface tensions of embryonic tissues predict their mutual envelopment behavior. Development **122**, 1611-20 (1996).
5. Steinberg, M. S. & Takeichi, M. Experimental specification of cell sorting, tissue spreading, and specific spatial patterning by quantitative differences in cadherin expression. Proc Natl Acad Sci U S A **91**, 206-9 (1994).
6. Krieg, M. et al. Tensile forces govern germ-layer organization in zebrafish. Nat Cell Biol **10**, 429-36 (2008).
7. Farhadifar, R., Roper, J. C., Aigouy, B., Eaton, S. & Julicher, F. The influence of cell mechanics, cell-cell interactions, and proliferation on epithelial packing. Curr Biol **17**, 2095-104 (2007).
8. Watanabe, G. et al. Protein kinase N (PKN) and PKN-related protein rhophilin as targets of small GTPase Rho. Science **271**, 645-8 (1996).
9. Amano, M. et al. Identification of a putative target for Rho as the serine-threonine kinase protein kinase N. Science **271**, 648-50 (1996).
10. Sahai, E. & Marshall, C. J. ROCK and Dia have opposing effects on adherens junctions downstream of Rho. Nat Cell Biol **4**, 408-15 (2002).
11. Lancaster, C. A. et al. Characterization of rhoGAP. A GTPase-activating protein for rho-related small GTPases. J Biol Chem **269**, 1137-42 (1994).
12. Moreno, E. Is cell competition relevant to cancer? Nat Rev Cancer **8**, 141-7 (2008).
13. Diaz, B. & Moreno, E. The competitive nature of cells. Exp Cell Res **306**, 317-22 (2005).

14. Dupre-Crochet, S. et al. Casein kinase 1 is a novel negative regulator of e-cadherin-based cell-cell contacts. Mol Cell Biol **27**, 3804-16 (2007).
15. Fujita, Y. et al. Hakai, a c-Cbl-like protein, ubiquitinates and induces endocytosis of the E-cadherin complex. Nat Cell Biol **4**, 222-31 (2002).
16. Capaldo, C. T. & Macara, I. G. Depletion of E-cadherin disrupts establishment but not maintenance of cell junctions in Madin-Darby canine kidney epithelial cells. Mol Biol Cell **18**, 189-200 (2007).
17. Hogan, C. et al. Rap1 regulates the formation of E-cadherin-based cell-cell contacts. Mol Cell Biol **24**, 6690-700 (2004).
18. Matzke, R., Jacobson, K. & Radmacher, M. Direct, high-resolution measurement of furrow stiffening during division of adherent cells. Nat Cell Biol **3**, 607-10 (2001).
19. Darling, E. M., Topel, M., Zauscher, S., Vail, T. P. & Guilak, F. Viscoelastic properties of human mesenchymally-derived stem cells and primary osteoblasts, chondrocytes, and adipocytes. J Biomech **41**, 454-64 (2008).
20. Darling, E. M., Zauscher, S., Block, J. A. & Guilak, F. A thin-layer model for viscoelastic, stress-relaxation testing of cells using atomic force microscopy: do cell properties reflect metastatic potential? Biophys J **92**, 1784-91 (2007).